IEICE Proceeding Series

On the Analysis of a Scaling Law Related to Random Walks -for the distributions of broken fragments of glass, areas enclosed by city roads, and divided faces in network models-

Yukio Hayashi

Vol. 1 pp. 106-109
Publication Date: 2014/03/17
Online ISSN: 2188-5079

2012 International Symposium on Nonlinear Theory and its Applications
NOLTA2012, Palma, Majorca, Spain, October 22-26, 2012

On the Analysis of a Scaling Law Related to Random Walks -for the distributions of broken fragments of glass, areas enclosed by city roads, and divided faces in network models-

Yukio Hayashi†

†Japan Advanced Institute of Science and Technology
1-1 Asahidai, Nomi-city, Ishikawa, 923-1292 Japan
Email: yhayashi@jaist.ac.jp

Abstract—A common distribution of areas (or mass) is observed in fragments of glass, city roads, and cracking patterns. In order to study a generation mechanism of the scaling law, we consider a fractal-like hierarchical network construction based on random divisions of rectangles. The stochastic process makes a Markov chain and corresponds to directional random walks with splitting into four particles. We derive a combinatorial analytical form and its continuous approximation for the distribution of rectangle areas, and show a good fitting with the actual distribution in the averaging behavior of the divisions.

1. Introduction

Scaling laws have been observed in complex systems. One of them, there is a common interesting characteristic; the frequency distributions have a fat-tail in fragment-size and -mass of glass [1][2], areas enclosed by city roads [3][4], and pore size/volume in random packings [5][6]. In particular, it is attractive that the distribution in fragmentation of glass is changed from a lognormal to a power-law-like according to low and high impacts [1], which determine the limitation of breakable sizes. For understanding the fundamental mechanism of such phenomena, we consider a spatial model based on random division process. As a scalable and distributed design method, we propose a geographical network construction [7] for load balancing in the adaptive change of node's territories assuming on a wireless communication environment. This planar network consisting of short links between no-hub nodes with small degrees is not the well-known scale-free network generated by a selfish "rich-gets-richer" rule, but a generalization of multi-scale quartered (MSQ) network model [8, 9] from the division of square limited as a self-similar tiling to that of rectangle. Therefore, it is both efficient and robust.

2. Generalized MSQ Network

We consider a two-dimensional $L \times L$ square, in which lattice points give the feasible setting positions of nodes. Initially, there exist only the outer square without lattice points. We propose the network construction as follows. At each time step, a rectangle is chosen uniformly at random (u.a.r), and it is divided into four smaller rectangles. For the division, vertical and horizontal axes are also chosen u.a.r from segments on the $L \times L$ square lattice. Then, the smaller rectangle with an area $x \times y$ (x, y denote the two edge lengths) is generated from the chosen rectangle with an area $x' \times y'$. Simultaneously, rectangles with the areas $x' - x \times y$, $x \times y' - y$, and $x' - x \times y' - y$ are generated. Here, each edge length $x, y \in Z_+$ is randomly chosen as a positive integer in $x + 1 \leq x' \leq L$ and $y + 1 \leq y' \leq L$. The case of $L \to \infty$ gives a general position for the division point.

The stochastic network generation makes a Markov chain. The state is represented by a vector $(n_{11}, \ldots, n_{xy}, \ldots, n_{LL})$, where n_{xy} denotes the number of rectangle with the area $x \times y$ (It is degenerately simplified in Fig. 1, when the difference of areas is ignored for discussing the distribution of layers in subsection 3.2). In particular, the emanative transition probability to divide a rectangle with the area $x \times y$ is not fixed but proportional to n_{xy} because of the uniformly at random selection of a face. In other words, the probability depends on a sequence of chosen rectangles during the transition before a final absorbing state for the indivisible width $x = 1$ or $y = 1$. Thus, we generate a hierarchical network that consists of subdivided rectangles.

3. Scaling Law of Area Distribution

3.1. Combinatorial Analysis

For the network construction, the recursive process can be regarded as a directional random walk of a particle with splitting into four copies, when a pair (x, y) of edge lengths of a rectangle is corresponded to the position of particle in the x-y coordinates, as shown in Fig. 2. A particle is randomly chosen at a time step, and moves toward smaller coordinate values from (x', y') to (x, y), where $x < x'$ and $y < y'$, until the

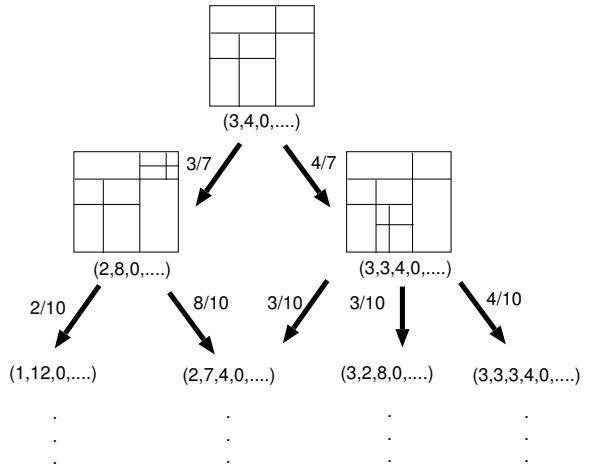

Figure 1: Branching tree diagram of the state vector $(n_1, n_2, \ldots)$ for the division processes, where n_l is the number of faces on the l-th depth. Each fraction denotes the transition probability.

boundary at $x = 1$ or $y = 1$.

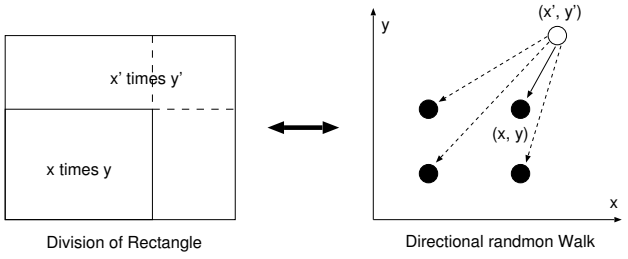

Figure 2: Correspondence between the division of a rectangle and the directional random walk with splitting.

The average behavior is described by the following system of difference equations for $2 \le x, y \le L-1$.

$$\Delta n_{xy} = -p_{xy} + \sum_{x',y'} \frac{4p_{x'y'}}{(x'-1)(y'-1)}, \qquad (1)$$

where Δn_{xy} is the average difference of n_{xy} in one step, and $p_{xy} \stackrel{\text{def}}{=} n_{xy} / \sum_{x">1y">1} n_{x"y"}$ is the existing probability of a particle at (x, y). The factor 4 in the numerator of right-hand side of Eq.(1) is due to feasible positions of the $x \times y$ at left/right and upper/lower corners in the division of $x' \times y'$. The denominator is the combination number for the relative positions of emanating particles in the intervals $[1, x'-1]$ and $[1, y'-1]$. The sum is taken over the integers $x+1 \le x' \le L$ and $y+1 \le y' \le L$ for a given (x, y).

From $\Delta n_{xy} = 0$ in Eq.(1), we have

$$p_{L-1L-1} = \frac{4p_{LL}}{(L-1)^2},$$

$$p_{xL-1} = p_{L-1y} = \frac{4p_{LL}}{(L-1)^2}, \quad x > 1, y > 1,$$

$$p_{L-2L-2} = \left(1 + \frac{4}{(L-2)^2}\right) \frac{4p_{LL}}{(L-1)^2}.$$

In general, we obtain the solution by applying the above in decreasing order of x and y recursively.

$$p_{xy} = \left\{ 1 + \sum_{\mathcal{P}} \left(\Pi_{i=1}^{l} \frac{4}{(x_i - 1)(y_i - 1)} \right) \right\} \frac{4p_{LL}}{(L-1)^2}, \qquad (2)$$

where $\sum_{\mathcal{P}}$ denotes the sum for a set of paths through the points $(x_1, y_1), (x_2, y_2), \ldots, (x_n, y_n)$, with $x_i, y_i \in Z_+$, $x < x_1 < x_2 < \ldots < x_i < \ldots x_l \le L-1$, and $y < y_1 < y_2 < \ldots < y_i < \ldots y_l \le L-1$ in all combinations of $l = 1, 2, \ldots \min\{L-1-x, L-1-y\}$.

By substituting the solution p_{xy} of Eq.(2) into the following right-hand sides,

$$\begin{aligned} n_{1y} &= \textstyle\sum_{x'>1, y'>y} \frac{4p_{x'y'}}{(x'-1)(y'-1)}, \\ n_{x1} &= \textstyle\sum_{x'>x, y'>1} \frac{4p_{x'y'}}{(x'-1)(y'-1)}, \\ n_{11} &= \textstyle\sum_{x'>1, y'>1} \frac{4p_{x'y'}}{(x'-1)(y'-1)}, \end{aligned}$$

we obtain the distribution $P(A)$ of rectangle area A. The sum is taken over the integers $x', y' \le L$, n_{11}, n_{x1}, and n_{1y} denote the number of the finally remaining rectangles with the areas 1×1, $x \times 1$, and $1 \times y$, which are no more divisible. Note that the unknown p_{LL} disappears by the numerator and the denominator in all of $P(1) = n_{11}/\mathcal{N}$ and $P(x) = (n_{x1} + n_{1x})/\mathcal{N}$, where $\mathcal{N} = n_{11} + \sum_{x''>1} n_{x''1} + \sum_{y''>1} n_{1y''}$ denotes the total number of the divided rectangle faces.

Figure 3 shows the distribution of areas with width one for $L = 10, 20, 50, 100, 200$, and 400 from left to right. Our solution denoted by lines is almost completely fitting with the actual distribution denoted by marks. In particular, a part of linear tail becomes longer, as L is larger. This phenomenon is similar to that in the fragment-size and -mass of glass [1][2], in which the distribution changes from a lognormal to a power-low-like according to low and high impacts.

3.2. Continuous Approximation

In order to analyze the distribution of areas for a large L, we approximate the process to be divisible at any positions on two edges of a rectangle, by ignoring the restriction to the segments on a $L \times L$ square lattice. For $l = 1, 2, \ldots$ until the maximum layer at a given time, the mixture distribution of p_l and $g_{2l}(\log A)$, which denote the frequencies of layer l and of area A in the layer l, are considered. We derive these frequencies separately.

First, we derive the distribution $p_l \stackrel{\text{def}}{=} n_l/\mathcal{N}$ of layers. As shown in [9] for the number n_l of faces in

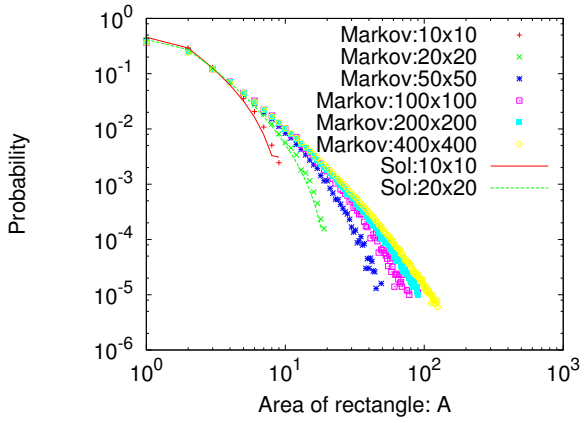

Figure 3: Distribution of areas with width one in the extreme rectangles generated from the initial $L \times L$ square. The marks titled "Markov" show the averaged results by 100 samples of the actual divisions of rectangles and the lines titled "Sol" show the solution for Eq(2).

the l-th layer, the averaging behavior of difference $\Delta n_l \stackrel{\text{def}}{=} n_l(t+1) - n_l(t)$ can be written to

$$\begin{aligned} \Delta n_l &= 3(t+1)p_l(t+1) - 3tp_l(t), \\ &= 3t[p_l(t+1) - p_l(t)] + 3p_l(t+1). \end{aligned}$$

Using $p_l(t+1) \approx p_l(t)$, we have

$$p_l(t+1) - p_l(t) = -\frac{4}{3t}\{p_l(t) - p_{l-1}(t)\}, \qquad (3)$$

where $p_0 \equiv 0$ is assumed for convenience.

We also derive the following expression [9] by using a model in interacting infinite particle system,

$$\begin{aligned} dn_l/d\tau &= 4n_{l-1} - n_l, \quad l \geq 2, \\ dn_1/d\tau &= -n_1. \end{aligned}$$

The solution is

$$n_l = \frac{(4\tau)^{l-1}}{(l-1)!}e^{-\tau}, \quad \mathcal{N}(\tau) = e^{3\tau},$$

$$p_l = \frac{(4\tau)^{l-1}}{(l-1)!}e^{-4\tau}, \qquad (4)$$

where τ has a logarithmic time scale from the relation $1 + 3t = e^{3\tau}$ of the total number of faces. Note that the solutions of Eq.(4) coincide with that of Eq.(3) asymptotically after a huge time [9].

Second, we consider a rectangle face at the l-th layer generated after some steps. Remember that the number l is defined by the division's depth. The area S_l is given by the product of shrinking rates $0 < X_i, Y_i < 1$, $i = 1, 2, \ldots, l$, for two edges of rectangle,

$$S_l = \Pi_{i=1}^{l} X_i Y_i L^2,$$

where X_i and Y_i is rational numbers, and S_l is a positive integer in the division process, strictly speaking.

As an approximation for a large L, we assume that the random variables X_i and Y_i follow a $(0, 1)$ uniform distribution. Then we define a variable $x \stackrel{\text{def}}{=} -\log(S_l/L^2) = -\sum_i(\log X_i + \log Y_i)$, $x \geq 0 \Leftrightarrow L^2 \geq S_l$, the probability of x follows a gamma distribution

$$g_{2l}(x) = e^{-x}\frac{x^{2l-1}}{(2l-1)!}. \qquad (5)$$

4. Numerical simulation results

We investigate the distributions decomposed into the approximative p_l and g_{2l}, and discuss the condition for a good fitting to each of components in the actual distributions for the divisions of rectangles.

Figure 4 shows the distribution p_l of layers at time steps $t = 50, 500$, and 5000. By the effect of width one, there exist a gap between the solution of difference equation(3) denoted by open marks and the actual distribution denoted by lines, although these distributions almost coincide in the MSQ networks based on a self-similar tilling [9]. The gap becomes slightly larger as L is smaller and t is larger, because the effect tends to appear in more coarse-grained divisions and a deeper layer. The Poisson distribution of Eq.(4) denoted by closed marks has a slightly larger gap than the solution of difference equation(3) denoted by closed marks in Fig. 4 and even in the MSQ networks. Figure 5 shows the cumulative distribution of $x = \log(L^2/A)$ restricted in the l-th layer. We chose the most observable layer $l = 5, 8, 11$, and 14, which correspond to the peaks of p_l at $t = 50, 500, 5000$, and 50000, respectively. Because the most observable layer is dominant in the mixture distribution $\sum_l p_l g_{2l}$. The effect of width one tends to appear as t is larger as shown in more right curves.

Between our approximation $\sum_l p_l g_{2l}$ by Eq.(3) and the the actual distribution of areas, we obtain a good fitting for $L = 10^8$ in Fig. 6(a) but remark a small gap for $L = 10^3$ in Fig. 6(b) The slope of -1 guided by the segment correspond to the exponents $-1.89 \sim -2$ of the frequency distributions for fragment-mass of glass [1] and areas enclosed by the city roads [3], because of the integral in the cumulative distribution.

5. Conclusion

We have considered a spatial network construction based on random divisions of rectangles for understanding the fundamental generation mechanism of the lognormal and power-law distributions of areas, which are commonly observed in fragments of glass, city roads, and cracking patterns. We have derived the exact solution for the extreme rectangles with width

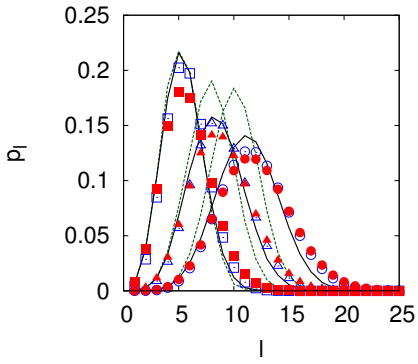

Figure 4: Distributions p_l of layers at time steps $t = 50, 500$, and 5000 from left to right. The black solid and green dashed lines correspond to the averaged result by 100 samples of the actual divisions of rectangles for $L = 10^8$ and $L = 10^5$, respectively. The open and closed marks correspond to the solution of Eq.(3) and Poisson distribution in Eq.(4).

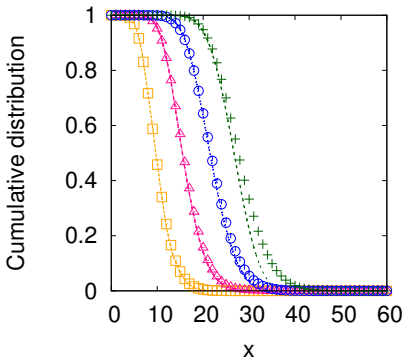

Figure 5: Cumulative distribution of x restricted in the layer l for $L = 10^8$ at time steps $t = 50, 500, 5000$, and 50000 from left to right. The lines show the averaged results for 100 samples of the actual divisions of rectangles, while the corresponding marks show the results for the gamma distribution $g_{2l}(x)$ of Eq.(5).

one on a combinatorial analysis, and also its continuous approximation for a large size. Simulation results show a good fitting of our approximation with the actual distribution of areas, especially for a large L in fine-grained divisions and at a small time t.

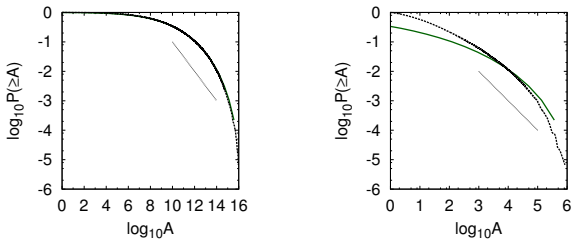

(a) $L = 10^8$ (b) $L = 10^3$

Figure 6: Cumulative distribution $P(\geq A)$ at $t = 500$. The green solid and black dashed lines show our approximation and the actual distribution, respectively.

Acknowledgment

The author would like to thank Y. Ide, T. Machida, and N. Konno for discussing the continuous approximation. This research is supported in part by a Grant-in-Aid for Scientific Research in Japan, No. 21500072.

References

[1] H. Katsuragi, D. Sugino, and H. Honjo, "Crossover of weighted mean fragment mass scaling in two-dimensional brittle fragmentation," *Phys. Rev. E*, 70, 065103, 2004.

[2] T. Ishii, and M. Matsushita, "Fragmentation of Long Thin Glass Rods," *Phys. Rev. E*, 61(10), 3474–3477, 1992.

[3] S. Lämmer, B. Gehlsen, and D. Helbing, "Scaling laws in the spatial structure of urban road networks," *Physica A*, 363, 89–95, 2006.

[4] S.H.Y. Chan, R.V. Donner, and S. Lämmer, "Urban road networks -spatial networks with universal geometric features?" *Euro. Phys. Journal B*, 84, 563–577, 2011.

[5] G.W. Delaney, S. Hutzler, and T. Aste, "Relation between grain shape and fractal properties in random Apollonian packing with grain rotation," *Phys. Rev. Lett.* **101**, 120602, 2008.

[6] P.S. Dodds, and J.S. Weitz, "Packing-limited growth of irregular objects," *Phys. Rev. E* **67**, 016117, 2003.

[7] Y. Hayashi, "Rethinking of Communication Requests, Routing, and Navigation Hierarchy on Complex Networks -for a Biologically Inspired Efficient Search on a Geographical Space-," In *Introduction to Routing Issues,* Arshin Rezazadeh(ed), iConcept Press, 2012.

[8] Y. Hayashi, and Y. Ono, "Geographical networks stochastically constructed by a self-similar tiling according to population," *Phys. Rev. E*, 82, 016108, 2010.

[9] Y. Hayashi, "An approximative calculation of the fractal structure in self-similar tilings," *IEICE Trans. Fundamentals*, E94-A(2), 846–849, 2011.